J. Fluid Mech. (1983), *vol.* 130, *pp.* 397–409
Printed in Great Britain

Transition of mechanically generated regular waves to wind waves under the action of wind

By MITSUHIKO HATORI† AND YOSHIAKI TOBA
Department of Geophysics, Faculty of Science, Tohoku University, Sendai 980, Japan

(Received 18 February 1982 and in revised form 9 December 1982)

The transition process of mechanically generated regular waves into wind waves is investigated in a wind-wave tunnel. Modulations of characteristic quantities of the waves are examined in both space and time using wave-gauge arrays. The transition begins with the occurrence of wave breaking, and it is associated with the following two processes: (i) the irregularization, i.e. the generation and amplification of a random modulation whose wave height and period are in phase; and (ii) the frequency shift to the lower side by the mutual coalescence of waves through the amplification of the modulation, the coalescence occurring at the troughs of the period modulation. The modulational properties under the effect of wind with wave breaking are thus in part different from the theoretical prediction of modulational instability of a freely travelling wavetrain. It is concluded that the mechanism of the transition is the modulational instability coupled with the wind effects.

1. Introduction

Several non-spectral models of wind waves, in which the effect of nonlinearity dominates, have recently been proposed by Lake & Yuen (1978), Ramamonjiarisoa & Mollo-Christensen (1979) and Hamilton, Hui & Donelan (1979). The essence of these models is to regard the wind wave as a modulated nonlinear water wavetrain with a single carrier wave. In particular, Lake & Yuen suggested the possibility of explaining the shift of frequency of wind waves to the lower side, based on the experimental evidence of Lake *et al.* (1977), who showed that a strongly modulated wavetrain accompanied by wave breaking shifts to a sideband mode of a lower frequency even in the absence of wind, in contrast with the recurrent nature of the theoretical prediction. A more detailed description of this phenomenon has recently been made by Su *et al.* (1982) and Melville (1982). They have confirmed experimentally the instability predicted by Longuet-Higgins (1978*a*, *b*; 1980) and Longuet-Higgins & Cokelet (1978), and described the relation between the onset of wave breaking and the unrecurrent frequency shift.

In wind waves, wave breaking is frequently observed, especially in short wind waves in a laboratory. Moreover, wind waves have a particular internal structure induced by the wind, which distinguishes them from a pure water wave (Toba *et al.* 1975). In fact, Okuda (1982*a–c*) has reported that there is a strongly vortical region, which is supported by the tangential stress at the crest of individual waves and which must be intimately coupled with the irrotational mode in the lower interior region. It is likely that the evolution of wind waves is greatly different from that of a nonlinear wavetrain because of this particular action of the wind.

To clarify the mechanism pertaining to wind waves, examination of the evolution

† Present address: Maizuru Marine Observatory, Shimofukui, Maizuru 624, Japan.

of water waves coupled with the action of the wind is useful, since the action of wind may be revealed in conditions where the properties of water waves themselves are much retained. As a precursor of the present study, Hatori, Tokuda & Toba (1981) conducted an experiment on the evolution of mechanically generated water waves under the action of wind, and reported that there are four stages in this evolution. Imai *et al.* (1981) further studied the passage from the first to the second stages, where the attenuation of local wind waves coexisting with regular waves and simultaneous growth of regular waves begin to take place. Toba *et al.* (1982) presented a further discussion. In the present study, we focus our attention on the fourth stage, which is the transition process of regular waves to wind waves.

As also shown by Mizuno (1975) and by Mollo-Christensen & Ramamonjiarisoa (1982), Hatori *et al.* (1981) showed that mechanically generated regular waves under the action of wind grow rapidly at a constant frequency until wave breakings occur (this is the third stage), and thereafter the transformation into irregular waves, i.e. wind waves, occurs. This transition is characterized by the following three properties: (i) wave breaking, (ii) increase of irregularity and (iii) low-frequency shift of regular waves. The transition stage is thus regarded as the stage where the regular waves acquire the nature of wind waves, and the above three items are the characteristic nonlinear properties of wind waves. The present study is a further step towards understanding wind-wave dynamics by focusing attention on the above particular points.

In the previous studies, the evolution of spectra at the transition stage was mainly discussed. In this paper attention is paid mainly to the evolution with fetch of modulational patterns of wave height, period and other characteristic quantities of individual waves, and differences between the sideband instability theory (Benjamin & Feir 1967) and the present results are pointed out. Mollo-Christensen & Ramamonjiarisoa (1982) have investigated the evolution of a modulated wavetrain by using bandpass filters. In this paper the occurrence of the mutual coalescence of waves is kinematically described in detail in connection with the evolution of modulational patterns in a wave field where the frequency shift is occurring.

2. Experiments and analyses

The experiments were performed in a wind-wave tunnel measuring 0.6 m in width, 1.2 m in height and 20 m in length, with a constant water depth of 0.6 m, as illustrated in Hatori *et al.* (1981). Regular waves were generated by a flap-type generator. All the records were collected in the stationary state, after at least 10 min of driving the fan and the wave generator. The originally generated regular wave was of frequency $f_R = 2.5$ Hz with wave height $H = 0.28$ cm. Because of the small steepness, 0.011, the regular waves under no wind preserved a periodic sinusoidal shape in the test section of the tunnel. The applied wind speed U was 10.0 m s^{-1} at the centre of the air inlet. The friction velocity, determined from the wind profile measured by a Pitot-static tube, was 0.59 m s^{-1} at fetch 7.8 m. The above experimental conditions are similar to those of Mizuno (1975) and Hatori *et al.* (1981). A regular wave of $f_R = 3.0$ Hz with $H = 0.19$ cm was also tested, and we arrived at the same conclusion.

The surface displacement was measured with capacitance-type wave gauges at three different combinations of measuring stations, listed in table 1 as cases (*A*), (*B*) and (*C*). Those of the case (*A*) were carried out to obtain an outline of the evolution with the fetch, and wave records were taken at seven stations from fetch 0.20 m to 14.00 m. The experiments in cases (*B*) and (*C*) were carried out to investigate the

Case		Station						
		a	*b*	*c*	*d*	*e*	*f*	*g*
(*A*)	Fetch (m)	0.20	1.85	3.85	5.85	7.85	10.85	14.00

		Station					
		1	2	3	4	5	6
(*B*)	Fetch (m)	3.97	4.97	5.97	6.97	—	—
(*C*)		—	—	5.97	6.97	7.97	8.97

TABLE 1. Three cases of measuring stations. In cases (*B*) and (*C*) each station has a pair of wave gauges separated by a distance of 25 cm. The fetches are the centre of these pairs. The measured section of (*B*) is from station 1 to 4 and (*C*) from station 3 to 6.

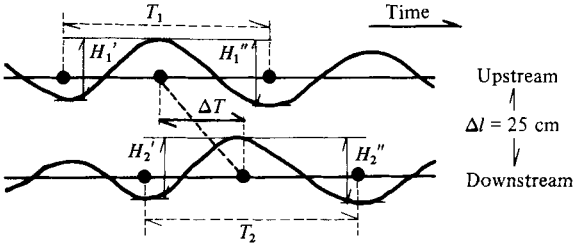

FIGURE 1. A schematic representation of the characteristic quantities of individual waves determined from time series of a pair of wave gauges separated at a distance of $\Delta l (= 25$ cm). Closed circles show the centres of the zero-crossing points. Wave height H is the mean of $H_1 = \frac{1}{2}(H_1' + H_1'')$ and $H_2 = \frac{1}{2}(H_2' + H_2'')$, period T is $T = \frac{1}{2}(T_1 + T_2)$, wave speed C is the propagation speed of the centre of a crest $\Delta l/\Delta T$, and wavelength L is estimated from $L = TC$.

transition stage in detail. In these two cases, four stations were located at intervals of 1.00 m. Each station had a pair of wave gauges placed at a distance of 0.25 m for detecting the wave speed and wavelength of individual waves. Case (*B*) used stations from fetch 3.97 m (station 1) to 6.97 m (station 4) and (*C*) from 5.97 m (station 3) to 8.97 m (station 6), with stations 3 and 4 overlapping. We examine the phase of increasing irregularity by (*B*) and that of low-frequency shift by (*C*).

Wave records were analysed by the following two methods: the usual spectral analyses, and the individual wave method used by Toba (1978) and Tokuda & Toba (1981). Power spectra were obtained by taking an average of 20 individual spectra. each of which was calculated by fast Fourier transform using 1024 digital data sampled every 0.02 s. The individual wave method was used for analysing the records of the cases (*B*) and (*C*). By utilizing this method, modulations of period, wave height, wavelength and wave speed were detected, and their evolutions with fetch were discussed. The definition of the characteristic quantities of individual waves is illustrated in figure 1.

In order to examine the relation between the evolution of regular waves and the wave breaking, the rate of wave breaking P was also measured. The value was defined by the probability of the occurrence of wave breaking while an individual wave propagates for a unit length (1 m). Breaking waves were identified by air bubbles entrained into the water. The number of individual waves observed for calculating P was about 1000.

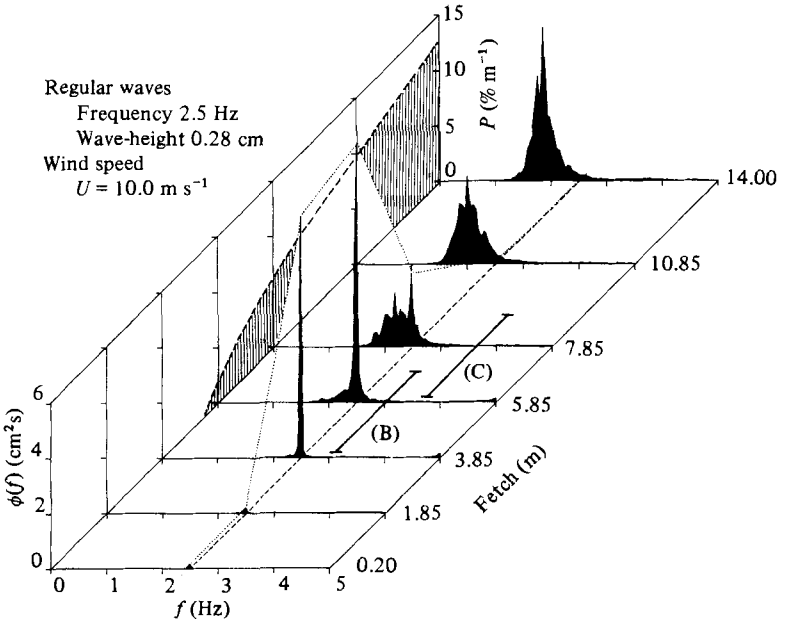

FIGURE 2. Evolution of power spectra for f_R = 2.5 Hz and U = 10.0 m s^{-1}. Shaded area indicates the rate of wave breaking P.

3. Results and discussion

3.1. *Outline of the transition*

We first describe briefly some specific features of the evolution of power spectra from the results of case (*A*) (figure 2). The energy of regular waves rapidly increases after fetch 1.85 m, and attains a saturation value at 3.85 m. After fetch 5.85 m, wave breaking begins, and the energy of regular waves rapidly decreases with simultaneous increase in the energy at frequencies lower than f_R. Finally, the power spectrum evolves into a structure similar to the wind waves at fetches 10.85 and 14.00 m. The spectral form at these two fetches is the same as the pure wind waves under the same wind condition. A similar evolutional process of spectra has been reported also in Mizuno (1975), Hatori *et al.* (1981) and Mollo-Christensen & Ramamonjiarisoa (1982).

Figure 2 clearly shows that the irregularity of regular waves increases after the occurrence of wave breaking, and finally the regular waves shift to wind waves of a lower frequency. Next, we will examine these two properties in detail on the basis of cases (*B*) and (*C*). The measured ranges in cases (*B*) and (*C*) are shown also in figure 2. Case (*B*) covers the phase of initial irregularization after the occurrence of wave breaking, where the peak frequency is constant, and (*C*) the phase of the lower frequency shift.

3.2. *Irregularization of regular waves by amplification of the modulation*

Figure 3 shows the wave records from station 1 (fetch 4 m) to station 4 (7 m), case (*B*). It is seen that a more-sinusoidal wavetrain at station 1 evolves into a much modulated wavetrain with the increasing fetch. We examine this deformation process of a wavetrain by using time series of characteristic quantities of individual waves.

The time series are obtained in the following manner. In case (*B*) the intervals of the wave gauges are 25 and 75 cm, as shown in figure 3, being 1 and 2.5 times the

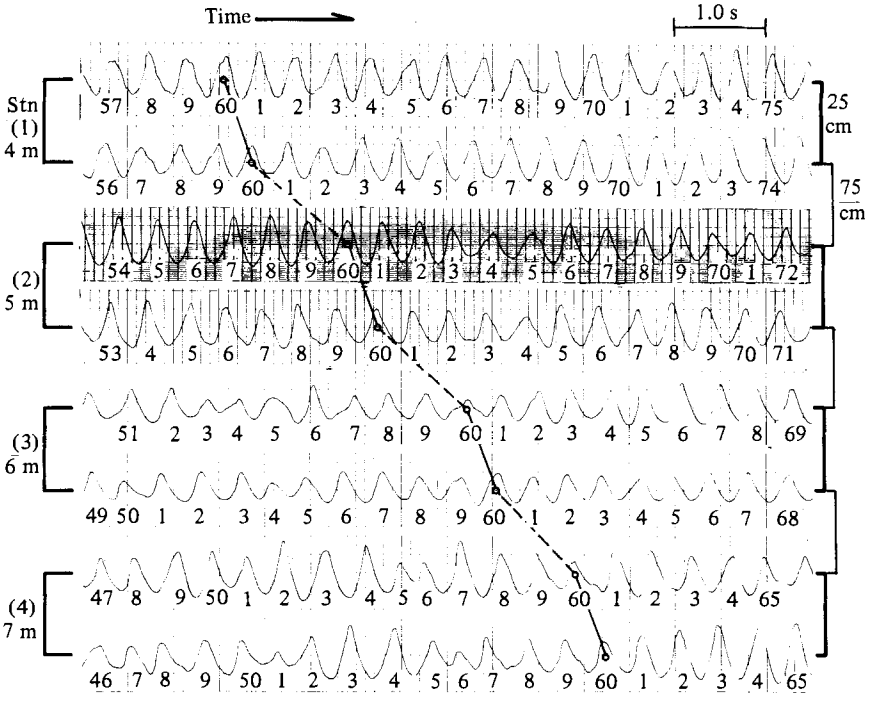

FIGURE 3. Example of a time series of case (*B*). A wave of the same number is the same individual wave. Dashed and smoothed lines show the evolution of an individual wave, no. 60.

mean wavelength 30 cm, so that the individual waves can be traced one after another in the records of 4 stations. Thus we can number the individual waves as shown in figure 3 taking wave no. 60 as an example. Series of characteristic quantities are obtained by plotting the values in numerical order for each station. The number of individual waves analysed is 100.

In addition to the modulational patterns of wave height, this simple analysis makes clear the development of modulational patterns of period, wavelength and others, which has not yet been examined in detail in previous experimental studies.

Figure 4 shows the time series of period T for stations 1–4. Thin dotted lines are smoothed patterns of the running mean calculated by a triangular filter with a bandwidth of 16 waves. Figure 4 indicates the following features. (i) Patterns of period modulation are rather random, but the modulation period of 5 to 6 wave periods is distinct. (ii) Most of the patterns propagate with fetch in the fetch direction but backwards relative to the individual waves as shown by dashed lines, indicating that the propagation speed is smaller than the wave speed of individual waves. It will be shown later that the travelling speed of the modulational patterns nearly coincides with the group velocity of water waves. (iii) Modulational patterns are amplified with an increase of fetch. (iv) Long-time variations in the smoothed patterns are not significant.

Similar features are also found in other quantities. Figure 5 shows the series of wave height H and wavelength L. As in the period, the modulational patterns are amplified with the fetch and propagate with a speed smaller than the wave speed. Long-time variations are more distinct than the case of the period. This long-time variation may be caused by the three-dimensional properties of the wave field in the wind-wave tank.

We can show that the propagation speed of the modulational patterns approximately

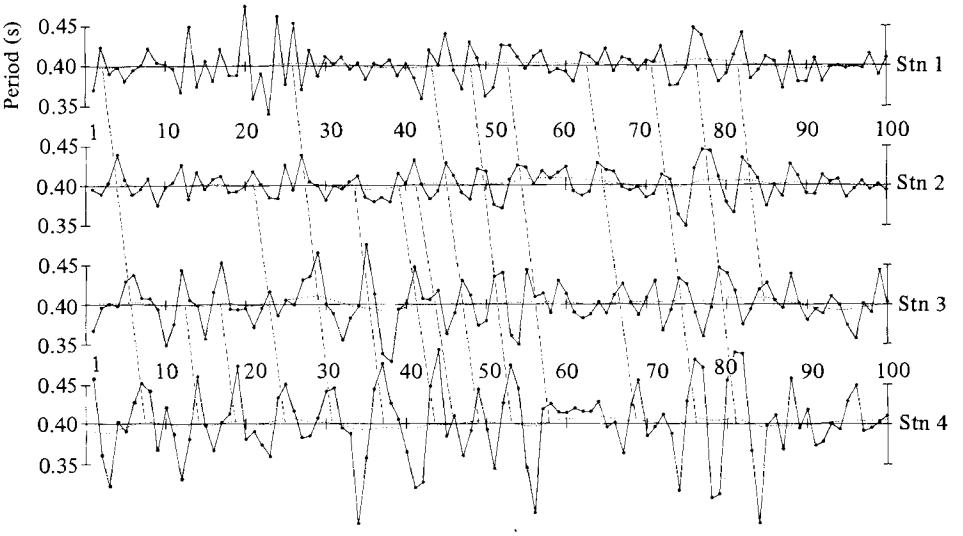

FIGURE 4. Series of period for the case (*B*). Horizontal axes are the number of individual waves. The dotted line indicates the running mean value, and the inclined broken lines show that the modulated property propagates with a definite speed (see the text).

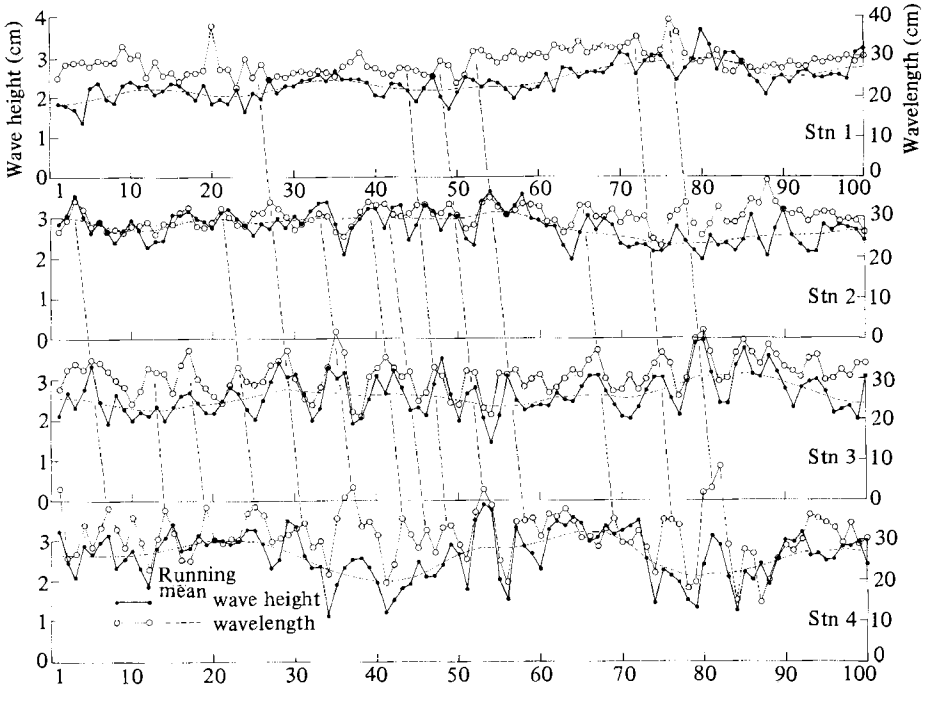

FIGURE 5. Series of wave height (small closed circles) and wavelength (large open circles). For other details see caption to figure 4.

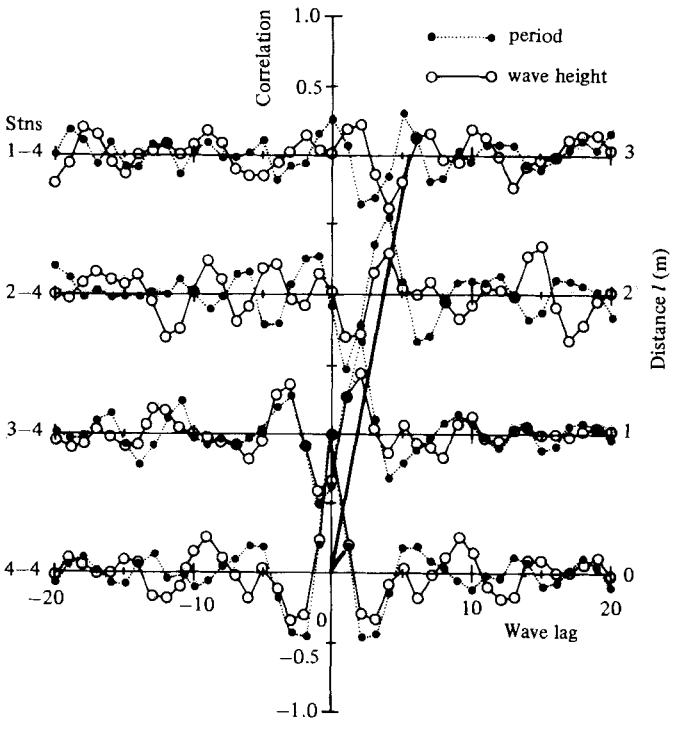

FIGURE 6. Space–time correlation functions of period (solid line) and wave height (dashed line). Horizontal axes are lags of waves. The two left numbers represent the two correlated stations. A solid line with an arrow shows the propagation direction of the maximum correlation coefficients.

coincides with the group velocity. Figure 6 shows space–time correlation functions of period and wave height. Horizontal axes are of the lag of wave, or indicate the time lag corresponding to the wave lag multiplied by the mean wave period. The propagation speed is found from a delay time of the maximum correlation. The line with an arrow in figure 6 shows the propagation direction of the maximum correlation. The velocity estimated from the inclination of this line is roughly 48 cm s^{-1}, which is slightly greater than the group velocity of the original regular waves of 40 cm s^{-1} when predicted as Stokes waves. Mollo-Christensen & Ramamonjiarisoa (1982) have also reported that modulation filtered in a band propagates at a speed greater than the group velocity. The excess propagation velocity may be interpreted as a special action of wind, since it is of the same order as the mean excess wave speed over Stokes waves of 4 cm.

Figure 6 indicates also that the maximum correlations decrease with an increase of the distance. This implies that the modulational patterns deform in the course of their propagation and amplification with the fetch. Figure 6 further shows that there is a difference in a degree of deformation among properties, that is, the correlation decreases more rapidly in the wave height than in the period. Changes in the maximum values of the correlations with the distance are shown in figure 7, which also shows the results for wavelength L, wave speed C, steepness $\delta(=H/L)$ and the excess wave speed over Stokes wave $u(=C-C_0)$, where C_0 is a wave speed of Stokes wave estimated from L and H. We find from the figure that the decrease of correlations is more rapid in H and C than in T and L. Correlations in δ and u decrease very rapidly to zero, indicating that δ and u are almost random.

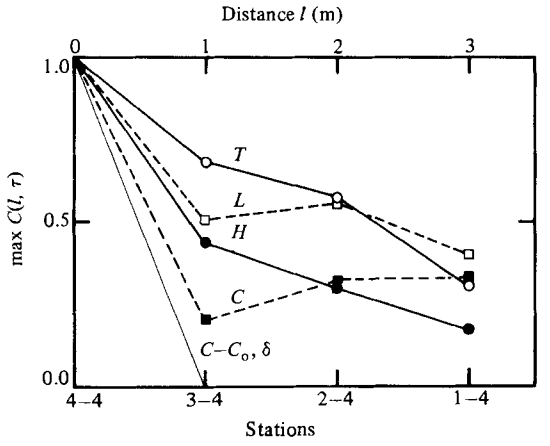

FIGURE 7. Changes of the maximum correlation coefficients with distance. Two numbers beneath the lower horizontal axis show the two correlated stations and the upper axis is the distance. Open circles are the period T, open squares the wavelength L, closed circles the wave height H and closed squares the wave speed C. A thin line shows the case of the excess wave speed $u(=C-C_0)$ and the steepness δ.

This result is interpreted as follows. The action of the wind will directly change the wave height through the energy input by its local work and through the energy dissipation by wave breaking, but the action is secondary for the wavelength, period and wave speed because the finite-amplitude dispersion effect is of the second order of steepness. Therefore the correlations decrease faster in H and δ than in T, L and C. The faster decrease of δ than H may be caused by the fact that δ is a combination of H and L. In figure 7 the correlation in C decreases in a similar degree to H. It may be associated with the randomness of u. The randomness of u strongly supports the idea that the abovementioned equivalent drift current in an average sense is not like a uniform drift current but a result of particular action of the wind, as discussed in Tokuda & Toba (1982).

The above-described characteristic features in the evolution of the modulational patterns are similar, in some aspects, to those of the modulational instability of a freely travelling water wavetrain studied by Benjamin & Feir (1967) and Lake *et al.* (1977). In fact, similarity exists in the following two points: (i) the observed mean modulational period of 5–6 wave periods approximately coincides with the theoretical prediction at the maximum instability of 4–5 wave periods; (ii) the observed growth rate of the standard deviations of T, H, L and C almost agrees with the theoretical prediction, and is 1.5 times the predicted maximum growth rate.

We can point out also some noticeable differences between the theory and the present results as follows. (i) The modulation is non-periodic (as in figures 4–6). In the theory the modulation is perfectly periodic by a selective amplification of a background noise, but the observed period of the individual modulational patterns is distributed within a range of from 2–10 wave periods and the amplitude of the patterns is different one from another. (ii) The modulational patterns are not necessarily amplified with the fetch (figures 4 and 5). (iii) The cross-correlations of the characterstic quantities of individual waves decrease with an increase of distance with different rates for the characteristic quantities (figures 6 and 7). (iv) The wavelength modulation and the wave-height modulation are, in most cases, in phase (figure 5), in contrast with the predicted phase angle between them, $\frac{1}{2}\pi$, at maximum instability. (v) A wave crest is not conserved, as will be investigated in §3.3.

The above five features imply that the influence of the wind is significant in the evolution of the modulational patterns. We have shown in §3.1 that wave breaking and irregularization, i.e. amplification of the modulational patterns, begin at the same time. The first feature, non-periodicity of the patterns, may be due to the amplification of the significant perturbations on a regular wavetrain generated by the wave breaking. The second and the third features may be partly connected with the deformation of the patterns by the wave breaking, while the third feature has already been discussed in the light of the wind action. The fourth feature shows that the mechanism of the modulational instability is not so effective in the amplification of the modulation. We suggest from the first to fourth features that the effects of the wind and the wave breaking play an important role in the evolution of the modulational patterns.

3.3. *Frequency shift by the mutual coalescence of waves*

The phase of low-frequency shift is examined from the experimental results of case (*C*). In a kinematical sense, the low-frequency shift can be regarded as the loss of a crest by the mutual coalescence of two adjoining waves. Figure 8 illustrates a typical coalescing process of two waves. At station 4 the waves, no. 37 and 38, are distinguishable, but at station 5 wave no. 37 becomes much smaller than no. 38. The interchange of wave scales between the upstream and the downstream records at station 5 is due to the dispersive nature of the wave field. Lastly they evolve into one wave at station 6, that is, one crest is lost, Mollo-Christensen & Ramamonjiarisoa (1982) also presented an example of this loss of crest in a wave record. We can now show that such a coalescence is connected with the amplification of modulational patterns described in the last section.

Figure 9 shows series of period as in figure 4. In the figure, the coalesced wave is divided into the following two kinds. One is the perfectly coalesced wave which has only one crest, e.g. nos. 37 and 38 at station 6 in figure 8. Large closed circles with arrows indicate the perfectly coalesced waves. The other is the wave which still has two crests in the sense of the peak-to-peak individual wave, but one crest in the zero-up-crossing individual wave, e.g. nos. 37 and 38 at station 5 in figure 8. In this case, the period of two waves distinguished by the peak-to-peak method is also illustrated by large open circles, together with the period by the zero-up-crossing method shown by large closed circles. Dashed lines show the propagation of the period modulation.

The most noticeable feature is that the coalescence occurs at the trough of the period modulation. The coalesced waves at station 6 are made up of two waves at the trough of the period modulation at station 5. This is also seen in the time series of figure 8, in which waves at the trough are surrounded by ellipses. The two waves at station 5, nos. 37 and 38, just before loss of a crest, are located at the trough. Another feature is that, just before the coalescence, waves around the coalescing waves have a constant period rather larger than that of the mechanically introduced waves (station 5 in figure 9). After the occurrence of coalescence, the period of the coalesced wave goes up to that of surrounding large waves, about 0.45 s, and the amplitude of the modulational patterns become small. This indicates that the mutual coalescence produces a somewhat *stabilized* wavetrain consisting of individual waves with a larger period than the introduced wave. It has been found that the above described features in the period modulation also hold in the modulation of wave height and wavelength.

A theoretical framework of the modulational theory (e.g. Chu & Mei 1971; Yuen

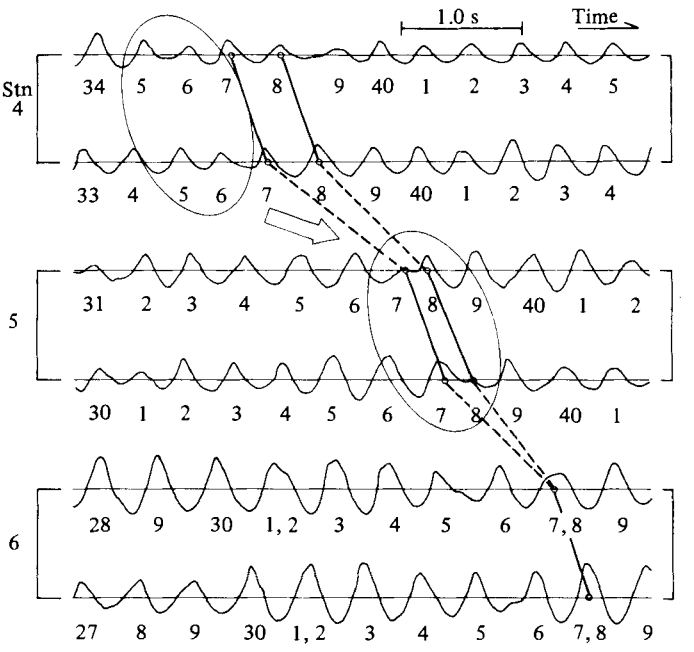

FIGURE 8. Typical time series showing the appearance of mutual coalescence, nos. 37 and 38 of case (*C*). Solid and dashed lines are the loci of the two waves. The ellipses show the trough of the period modulation.

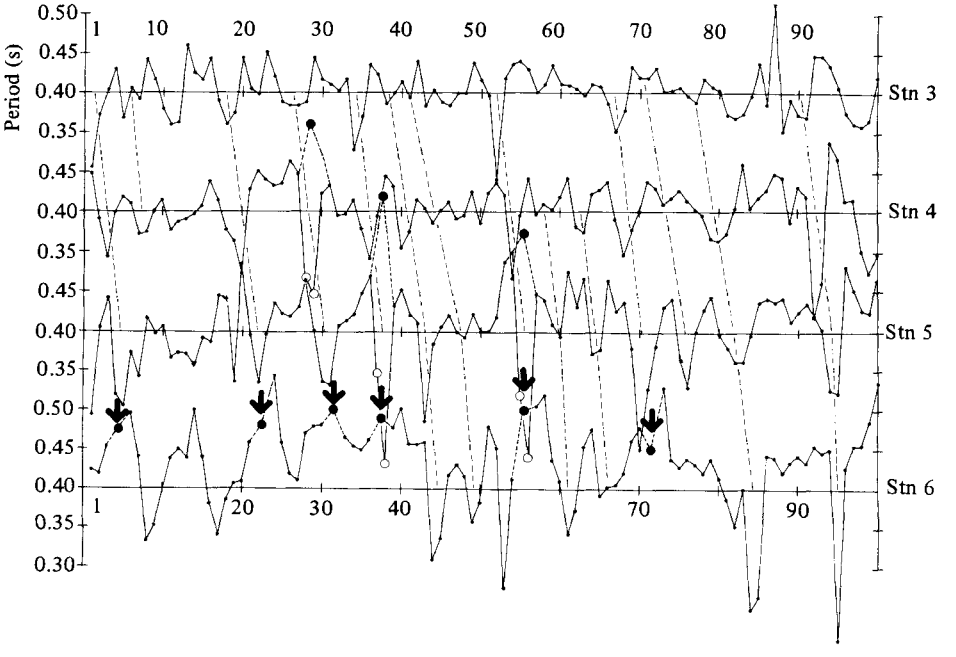

FIGURE 9. Series of period T for case (*C*). Large closed circles with arrows represent the perfectly coalesced waves which have only one crest, and other large closed circles the waves which still have two crests in the peak-to-peak analysis. The periods of two waves distinguished by the peak-to-peak analysis are shown by large open circles. The horizontal axes and the inclined broken lines are the same as figure 4.

& Lake 1975), which stands on the conservation of wave crests, cannot account for the coalescence. It seems that the mutual coalescence is essential in the mechanism of the low-frequency shift. As in the amplification of the modulation, it is considered that the coalescence is associated with the wave breaking. This idea is supported by experimental results for pure mechanical waves by Lake *et al.* (1977), Su *et al.* (1982) and Melville (1982), in which a strongly modulated wavetrain shifting to a lower-frequency mode was accompanied by wave breaking.

Finally, we refer briefly to the evolution of spectra at the transition stage in the light of the above-described results. As a consequence of the amplification of the modulational patterns whose mean period is 5–6 wave periods and whose wave height and period are in phase, the energy increase occurs mainly at lower frequencies around $\frac{4}{5}f_R$ or $\frac{5}{6}f_R$ (= 2.0 or 2.1 Hz), with a frequency jump of 0.5–0.4 Hz, if it is assumed that one crest is lost from every wave group. The spectrum at fetch 7.85 m in figure 2 clearly shows this situation. The value of the frequency jump is also similar to the experiments by Su & Bergin (1981) for purely mechanical waves.

4. Summary and concluding remarks

The present results are summarized as follows. The transition of regular waves into wind waves is associated with the following processes. The first is irregularization by the amplification of the modulational patterns whose wave height and period are mostly in phase, the irregularization and the wave breaking beginning at the same time. The second is the low-frequency shift by the mutual coalescence of individual waves through the amplification of the modulation. The above evolutional processes are similar in part to the prediction of the modulational instability theory, but different from the theory in several points.

We give here some further discussion on the possible causes other than wave breaking for the difference from the theory. Mollo-Christensen & Ramamonjiarisoa (1982) have estimated the orders of magnitude of terms of a nonlinear Schrödinger equation incorporating the effect of variable current, and have demonstrated that even weak disturbances in, say, a wind-induced current can cause a significant effect on the modulational dynamics of surface waves. In the present experiment, the excess wave speed over the Stokes-wave speed u changes randomly along the modulated wavetrain, and the standard deviation of u is 4–9 % of the mean wave speed, giving an effect comparable to the finite-amplitude effect. The results of our experiment seem to support the inference by Mollo-Christensen & Ramamonjiarisoa (1982). In recent laboratory observation of the internal flow structure of wind waves, Okuda (1982*a–c*) has shown the existence of a strongly vortical region near the wave crest and its non-uniformity and unsteadiness along the train of wind waves. These non-uniform and unsteady flow structures will cause the abovementioned variation of u along the wavetrain.

A further effect of the wind is the deformation of the wave profile. Forward-skewed profiles of wind waves are frequently observed in a wind-wave tunnel, as studied e.g. by Koga (1982). Masuda & Kuo (1981) have recently verified by comparison of bispectra of wind waves and of freely travelling random waves that the forward-skewed profiles of wind waves are due to the wind action. In the present experiments, the crests analysed in case (*B*) incline forwards by 13° from the symmetrical Stokes wave on average. This must introduce an alteration of the modulational instability theory. In any case, we must construct a model of the evolution of the modulated wavetrain

which includes the above-described wind effects as well as the finite-amplitude effect, and also includes the non-conservation of wave crests.

Lake & Yuen (1978) proposed a model of wind waves based on the nonlinear modulated wavetrain under no wind. However, our results show the crucial importance of the effects of the wind. The concept obtained from the present experimental results may be extended to the evolutional process of wind waves as follows. In the wind waves, the two phases of the amplification of the modulation and of the mutual coalescence of waves are coexistent, and the evolution process is maintained by the balance between the two phases. Evidence in favour of this view has been obtained by an experiment on pure wind waves. The description of this will be reported elsewhere.

The authors wish to express their thanks to the late Dr S. Kawai, Dr K. Okuda and other members of the laboratory for discussions during the course of this study. The authors are also indebted to Mr Y. Iami, now at the Kokusai Kogyo Co. Ltd, for his assistance in the experiment. This study was partially supported by the Grant-in-Aid for Scientific Research from the Ministry of Education, Science and Culture, Project no. 56116006.

REFERENCES

BENJAMIN, T. B. & FEIR, J. E. 1967 The disintegration of wave trains on deep water. Part 1. Theory. *J. Fluid Mech.* **27**, 417–430.

CHU, V. H. & MEI, C. C. 1971 The non-linear evolution of Stokes waves in deep water. *J. Fluid Mech.* **47**, 337–351.

HAMILTON, J., HUI, W. H. & DONELAN, H. A. 1979 A statistical model for groupiness in wind waves. *J. Geophys. Res.* **84**, 4875–4884.

HATORI, M., TOKUDA, M. & TOBA, Y. 1981 Experimental study on strong interaction between regular waves and wind waves – I. *J. Oceanogr. Soc. Japan* **37**, 111–119.

IMAI, Y., HATORI, M., TOKUDA, M. & TOBA, Y. 1981 Experimental study on strong interaction between regular waves and wind waves – II. *Sci. Rep. Tohoku Univ.* 5 (*Tohoku Geophys. J.*), **28**, 87–103.

KOGA, M. 1982 Characteristics of breaking wind-wave field in the light of individual wind-wave concept. (Unpublished manuscript.)

LAKE, B. M. & YUEN, H. C. 1978 A new model for nonlinear wind waves. Part 1. Physical model and experimental evidence. *J. Fluid Mech.* **88**, 33–62.

LAKE, B. M., YUEN, H. C., RUNGALDIER, H. & FERGUSON, W. E. 1977 Nonlinear deep-water waves: theory and experiment. Part 2. Evolution of the continuous wave train. *J. Fluid Mech.* **83**, 49–74.

LONGUET-HIGGINS, M. S. 1978*a* The instabilities of gravity waves of finite amplitude in deep water. I. Superharmonics. *Proc. R. Soc. Lond.* **A360**, 471–488.

LONGUET-HIGGINS, M. S. 1978*b* The instabilities of gravity waves of finite amplitude in deep water. II. Subharmonics. *Proc. R. Soc. London.* **A360**, 489–505.

LONGUET-HIGGINS, M. S. 1980 Modulation of the amplitude of steep wind waves. *J. Fluid Mech.* **99**, 705–713.

LONGUET-HIGGINS, M. S. & COKELET, E. D. 1978 The deformation of steep surface waves on water. II. Growth of normal-mode instabilities. *Proc. R. Soc. Lond.* **A364**, 1–28.

MASUDA, A. & KUO, Y.-Y. 1981 Bispectra for the surface displacement of random gravity waves in deep water. *Deep-Sea Res.* **28A**, 223–237.

MELVILLE, W. K. 1982 The instability of deep-water waves. *J. Fluid Mech.* **115**, 165–185.

MIZUNO, S. 1975 Growth of mechanically generated waves under a following wind I. *Rep. Res. Inst. Appl. Mech. Kyushu Univ.* **22**, 357–376.

MOLLO-CHRISTENSEN, E. & RAMAMONJIARISOA, A. 1982 Subharmonic transition and group formation in a wind wave field. *J. Geophys. Res.* **87**, 5699–5717.

OKUDA, K. 1982*a* Internal flow structure of short wind waves. I. On the internal velocity structure. *J. Oceanogr. Soc. Japan* **38**, 28–42.

OKUDA, K. 1982*b* Internal flow structure of short wind waves. II. The streamline pattern. *J. Oceanogr. Soc. Japan* **38**, 313–322.

OKUDA, K. 1982*c* Internal flow structure of short wind waves. III. Pressure distributions. *J. Oceanogr. Soc. Japan* **38**, 331–338.

RAMAMONJIARISOA, A. & MOLLO-CHISTENSEN, E. 1979 Modulation characteristics of sea surface waves. *J. Geophys. Res.* **84**, 7769–7775.

SU, M.-Y., BERGIN, M., MARLER, P. & MYRICK, R. 1982 Experiments on nonlinear instabilities and evolution of steep gravity-wave trains. *J. Fluid Mech.* **124**, 45–72.

TOBA, Y. 1978 Stochastic form of the growth of wind waves in a single-parameter representation with physical implications. *J. Phys. Oceanogr.* **8**, 494–507.

TOBA, Y., TOKUDA, M., OKUDA, K. & KAWAI, S. 1975 Forced convection accompanying wind waves. *J. Oceanogr. Soc. Japan* **31**, 192–198.

TOBA, Y., HATORI, M., IMAI, Y. & TOKUDA, M. 1982 Experimental study on elementary processes in wind waves using wind over regular waves. In *Proc. IUCRM Symp. on Wave Dynamics and Radio Probing of the Ocean Surface*, 13–20 *May* 1981, *Miami Beach* (to be published).

TOKUDA, M. & TOBA, Y. 1981 Statistical characteristics of individual waves in laboratory wind waves. I. Individual wave spectra and similarity structure. *J. Oceanogr. Soc. Japan* **37**, 243–258.

TOKUDA, M. & TOBA, Y. 1982 Statistical characteristics of individual waves in laboratory wind waves. II. Self-consistent similarity regime. *J. Oceanogr. Soc. Japan* **38**, 8–14.

YUEN, H. C. & LAKE, B. M. 1975 Nonlinear deep water waves: Theory and experiment. *Phys. Fluids* **18**, 956–960.